

Imaging features of mandibular squamous cell carcinoma in a cat

Beeldvormingskarakteristieken van squameus celcarcinoom van de mandibula bij een kat

¹M.M.W.M. Dekkers, ¹K. Kromhout, ¹J.H. Saunders, ¹S. David, ²G.Vercauteren, ¹E. Stock.

¹Department of Morphology, Imaging, Orthopedics, Rehabilitation and Nutrition, Faculty of Veterinary Medicine, Ghent University, Salisburylaan 133, 9820 Merelbeke, Belgium

²Zoolyx Veterinary Laboratory Services, Groeneweg 17, 9320 Aalst, Belgium

Moniek.Dekkers@UGent.be

ABSTRACT

A fourteen-year-old, neutered, male European Shorthair cat was referred with clinical signs of anorexia, weight loss and right sided mandibular swelling, which progressively increased in size. In addition, marked thickening and ulceration of the ipsilateral mandibular gingiva were both found. A computed tomography scan revealed marked amorphous periosteal reaction, extensive cortical disruption, moth-eaten to permeative osteolysis and moderate surrounding soft tissue swelling. The histopathological diagnosis was a grade 2 squamous cell carcinoma with infiltration in the bone and separation of bony trabeculae.

SAMENVATTING

Een veertienjarige, mannelijke, gecastreerde Europese korthaar werd doorverwezen met klinische klachten van anorexie, gewichtsverlies en een zwelling ter hoogte van de rechter mandibula die progressief toenam in grootte. Daarnaast vertoonden de mandibulaire gingiva een duidelijke verdikking en ulceratie. Een computertomografische scan toonde een uitgesproken amorfe periostale reactie, uitgebreide corticale onderbreking en 'door motten aangevreten' tot permeatieve osteolyse. De laesie was omgeven door een matige wekedelenzwelling. De histopathologische diagnose was een graad 2-plaveiselcelcarcinoom met infiltratie in het bot en onderbreking van de benige trabeculae.

INTRODUCTION

Approximately 10% of all feline tumors are intra-oral neoplasms, most of which are malignant (Stebbins et al., 1989; Liptak et al., 2007). More than 50% of these malignant tumors are squamous cell carcinomas (SCC) (Stebbins et al., 1989; Harvey and Emily, 1993). Oral and sinonasal SCC originate from the stratified squamous epithelium of the mucosa and are classified as keratinocyte tumors (Murphy et al., 2020). Commonly, these tumors arise from oral mucosa such as the gingiva and intraoral mucosa (Bilgic et al., 2015). The presentation of a SCC varies among different intraoral regions, sectioned into mandibular, maxillary, and lingual/sublingual areas, as described

below. When located at the mandible, the SCC are commonly described as proliferative, expansile and firm masses, while a maxillary SCC commonly presents as an ulcerative lesion with marked osteolysis, especially when located in the caudal maxillary region (Bilgic et al., 2015). Crater-like destruction of the maxillary palatine process, the incisive bone and zygomatic arch is often detected with invasion into the nasal cavity and decreased retropulsion of the ipsilateral eye (Bilgic et al., 2015; Supsavhad et al., 2016). A second different imaging feature is seen when comparing periosteal reaction between mandibular and maxillary SCC. The mandible-associated SCC shows solid/lamellar, irregular and speculated features, while more severe, irregular periosteal reac-

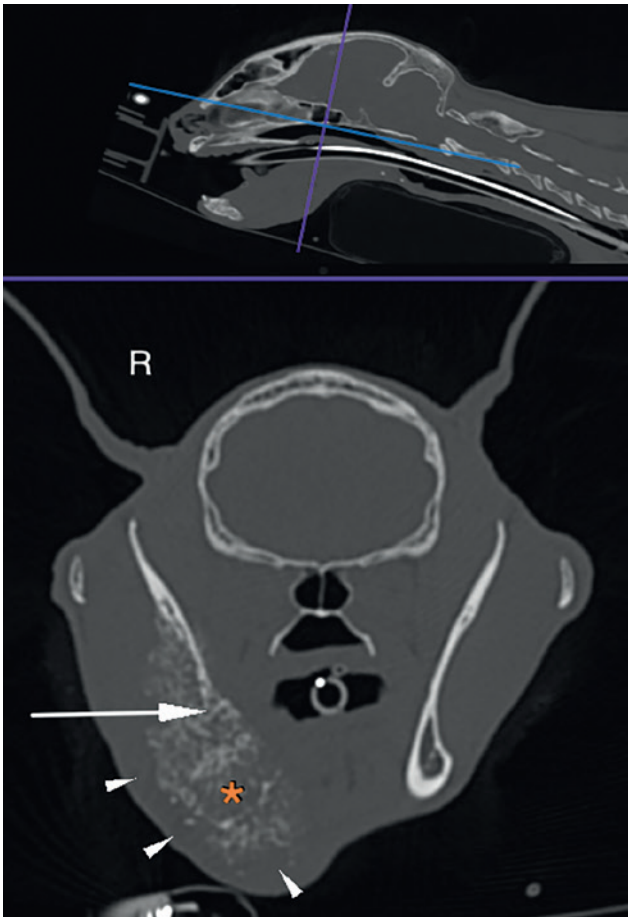


Figure 1. Transverse image, with reference slices on the upper sagittal image, in bone window showing an expansile bone lesion characterized by amorphous periosteal reaction (white arrowheads), extensive loss of cortical margin (white arrow) and moth-eaten osteolysis (orange asterisk).

tion has been detected in maxillary SCC (Strohmayr et al., 2020). A similar finding in both mandibular and maxillary SCC can be mobile or loss of teeth in the affected area, which has been reported to be more severe in case of ulcerative SCC (Bilgic et al., 2015). A lingual or sublingual SCC can have multiple presentations, namely ulcerative, necrotic, infiltrative or proliferative (Bilgic et al., 2015). Invasion of the tongue musculature is often present, causing diffuse and firm thickening of the tongue (Bilgic et al., 2015). In general, and regardless of the location, feline oral SCC are malignant neoplasms with an invasive character and poor margination (Bilgic et al., 2015; Strohmayr et al., 2020). General physical and oral examination cannot differentiate all these above-described characteristics, and differentiation between surrounding edema, inflammation, desmoplasia and tumor invasion cannot be made (Gendler et al., 2010). To effectively plan potential treatment approaches and assess the extent and invasiveness of the lesions, diagnostic imaging is imperative.

Radiographs reveal bone lysis, periosteal proliferation and soft tissue swelling in severe cases, but they have limitations in assessing extent and invasiveness (Pavlin et al., 2018). Thoracic radiographs are valuable for screening thoracic metastasis, with detectability limited to nodules of approximately 7 to 9 mm (Nemanic et al., 2006).

Ultrasound in the oral region faces challenges such as acoustic shadowing and reverberation artifacts. Its practical use includes assessing lymph nodes and determining the sentinel lymph node with contrast media, providing an option for surgical removal. Detection of intrapulmonary metastasis with ultrasound is viable only with peripheral nodules due to reverberation artifacts.

Magnetic resonance imaging (MRI) is preferred for soft tissue assessment, offering insights into invasion and tumor extension. However, its application in SCC is less documented, and it presents challenges compared to computed tomography (CT) in evaluating bone lysis and proliferation. MRI cannot assess intrapulmonary metastasis, and it is worth noting that thoracic MRI is not a standard procedure in veterinary medicine.

The imaging method of choice for oral SCC evaluation is contrast-enhanced CT with sentinel lymph node mapping. This combines bone and soft tissue assessment, contrast enhancement, detection of metastases and the sentinel lymph node(s). Contrast-enhanced CT can detect intrapulmonary metastasis with nodules as small as 2-3 mm, emphasizing its importance in thoracic evaluation. Additionally, it uniquely identifies oral SCC without a mass effect (Gendler et al., 2010). Precontrast CT features of oral SCC include an isoattenuating mass with associated osteolysis in 50% of the cases (Gendler et al., 2010). In 50 to 100% of the cases, mandibular SCC in cats is polyostotic (Gendler et al., 2010; Strohmayr et al., 2020). In postcontrast CT images, a SCC shows marked contrast enhancement in all cases with heterogeneous contrast enhancement as a predominant enhancement pattern (Gendler et al., 2010). Marked contrast enhancement is due to the highly vascular nature of SCC, which is a consistent finding in tumors that originate in the oral cavity in cats (Stebbins et al., 1989). The heterogeneous contrast enhancement pattern on CT images of SCC in cats has been suggested to represent tumor necrosis, desmoplasia or both (Sigal et al., 1996; Gendler et al., 2010).

The imaging features in this case exhibit similarities with those described in a case report of a benign hamartoma in a cat (Takagi et al., 2018). Vascular hamartoma, a benign congenital lesion, originating from disorganized mature vascular cells (Smith et al., 2010). The primary aim of this case report was to highlight the imaging characteristics of SCC in felines and to compare them with those of a benign hamartoma showing similar imaging features (Takagi et al., 2018).

CASE DESCRIPTION

History

A fourteen-year-old, neutered, male European Shorthair cat was referred with clinical signs of a two/three-week period of gradual hyporexia progressing to a one-day episode of total anorexia, weight loss, and right-sided mandibular swelling, progressively increasing in size. The latter had been diagnosed by the referring veterinarians two weeks earlier. Furthermore, the cat was known with hyperthyroidism which had been diagnosed ten months earlier and was well-controlled with oral drugs (Levamisole 1.25 mg twice a day).

General physical and oral examination

The general physical examination revealed a non-displaceable mass on the right mandible which extended from the level of the canine tooth to the caudal aspect of the right mandibular ramus and crossed the midline towards the left side. Furthermore, a mass-effect was visible displacing the tongue towards the left side. Finally, a systolic cardiac murmur 3/6 with punctum maximum at the left apex was also noted.

Medical imaging

Given the systolic heart murmur, an echocardiogram was performed which revealed severe hypertrophy of the left ventricle wall and mitral valve insufficiency due to dynamic left ventricular outflow tract obstruction with systolic anterior motion of the mitral valve. The left atrium was considered normal in size.

After the echocardiogram, the cat was premedicated intravenously using butorphanol (0.3mg/kg) and midazolam (0.2mg/kg) and general anesthesia was induced using propofol to effect (total dose of 3.5mg/kg). A CT (Toshiba Aquillon ONE TSX-301C) study of the head, neck, thorax, including part of the cranial abdomen, was performed. This revealed an expansile bone lesion affecting a large portion of the right mandible, extending from the apical aspect of the tooth root of Triadan 404 till the ventral aspect of the coronoid process at the mandibular ramus. Caudally, the lesion included the right angular and the right condylar process, till the level of the right temporomandibular joint. Marked amorphous periosteal reaction, extensive cortical disruption and moth-eaten to permeative osteolysis were identified (Figures 1, 2 and 3). There was almost complete lysis of the lingual and buccal cortical surfaces of the right mandible, as well as the lamina dura of Triadan 405 through 411, resulting in mobility of the teeth. Notably, the right mandibular teeth showed no displacement when compared to the opposite side.

Postcontrast CT images showed heterogeneous contrast enhancement of the right masseter muscle, the right lateral and medial pterygoid muscles and

the subcutaneous soft tissues lateral and medial to the right mandible (Figure 4). The regional lymph nodes were within normal limits and there was no evidence of intrathoracic metastatic disease.

Imaging findings identified a monostotic, expansile, aggressive mixed osteolytic and osteoproliferative bone lesion involving the right mandible without evidence of metastasis. Possible differentials were primary bone tumor (i.e. osteosarcoma, chondrosarcoma, multilobular osteochondrosarcoma) or soft tissue neoplasia (i.e. SCC, fibrosarcoma) with secondary bone involvement. Non-neoplastic diseases such as vascular hamartoma or chronic osteomyelitis were deemed less likely.

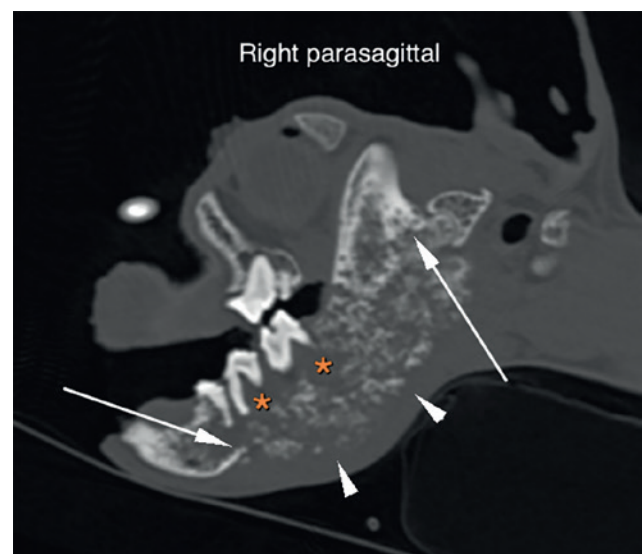


Figure 2. Parasagittal reconstruction (right) centered on the right mandible in bone window showing an expansile bone lesion characterized by amorphous periosteal reaction (white arrowheads), extensive loss of cortical margin (white arrows) and moth-eaten osteolysis (orange asterisks). Rostral is located to the left on the parasagittal image.



Figure 3. Three-dimensional surface rendering model of the right side of the skull.

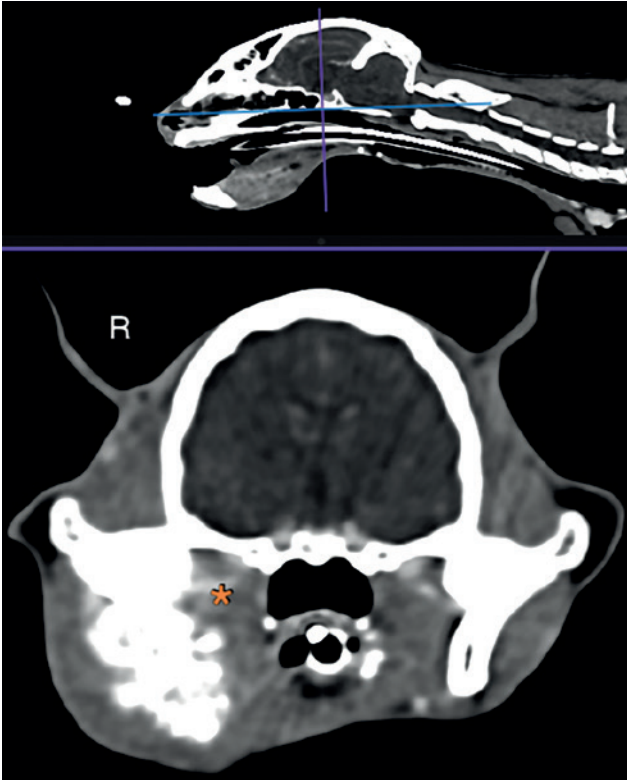


Figure 4. Transverse postcontrast reconstruction, with reference slices on the upper sagittal image, in soft tissue window with mild heterogeneous contrast enhancement at the level of the right pterygoid muscle (orange asterisk).

Histopathology

Due to the severity and extent of the lesion and poor prognosis of hemimandibulectomy in cats, the owners elected euthanasia. Postmortem histopathology (Zoolyx Veterinary Laboratory Services) of the mass revealed a disorganized infiltration of nests and trabeculae of the large polygonal cells with abundant eosinophilic cytoplasm, round nucleus with coarsely granular to vesicular chromatin and single prominent nucleolus embedded in ample highly cellular collagenous stroma. Anisocytosis and anisokaryosis were marked; several multinucleated cells were identified and mitoses, including a few atypical mitotic figures, were present: 6 per HPF (0.237 mm²). There was frequent central keratinization often associated with neutrophilic infiltration. On immunohistochemistry, neoplastic cells strongly expressed pancytokeratin (Anti-Pan Keratin AE1/AE3; an epithelium-specific-antibody). An epithelial tumor with squamous differentiation, desmoplastic response and bone invasion, compatible with a SCC was diagnosed (grade 2 based on invasive front grading system). There were both ulcerated and intact mucosal surfaces present. In the ulcerated areas the neoplastic cells reached the ulcerated mucosal surface. Under the intact mucosal surfaces, the neoplasm was located between the striated muscle fibers. Nests of tumoral cells were also found

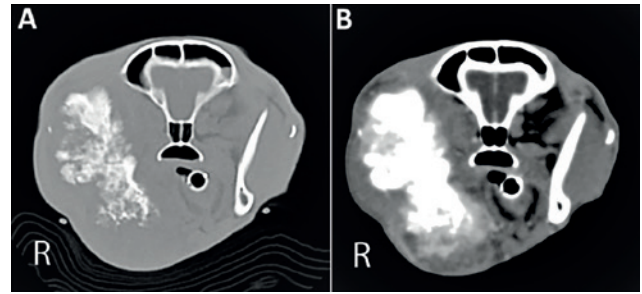


Figure 5. A. Computed tomography findings at bone window and B. Postcontrast soft tissue window of a mandibular vascular hamartoma. A substantial section of the central portion of the right mandibular bone was involved. In the postcontrast image, marked heterogeneous contrast enhancement can be appreciated (Takagi et al., 2018).

to infiltrate areas of well-differentiated (preexisting) bone with separation of bony trabeculae and with multifocal areas of osteonecrosis (osteolysis).

DISCUSSION

The presentation of SCC varies between intraoral regions. In the present mandibular-origin case, contrary to typical presentations, ulcerative lesions were present, and neoplastic cells reached the ulcerated mucosal surface. The periosteal reaction was severe, irregular and amorphous, deviating from the solid or lamellar pattern. A possible explanation for ulcerations in this case involves substantial mass expansion and infiltration into adjacent tissues, likely stemming from a delayed diagnosis of the SCC. A second explanation can be tumor type. The histopathologic grade of 2 indicates accelerated growth and increased infiltration compared to grade 1 tumors (Dissanayake, 2017) (Table 1).

The case exhibits imaging similarities with a benign hamartoma (Takagi et al., 2018). In Figure 5, an instance of a mandibular vascular hamartoma showing striking similarities to the present case is illustrated. Vascular hamartoma, likely originating from disorganized vascular cells, forms a tumor-like mass with severe bone proliferation, bone resorption and intense soft tissue contrast enhancement. The intense contrast enhancement could serve as a potential distinguishing imaging characteristic between a hamartoma and a SCC. However, it is essential to note that this conclusion is derived from a single case report. In addition to the potential contrast enhancement differences, the clinical presentation between these two entities may also differ. In the case of vascular hamartoma, the cat presented with hypersalivation and oral bleeding. Anorexia manifested only during episodes of oral bleeding but the cat recovered in between (Takagi et al., 2018). Due to these minor differences between the two types of lesions, biopsy is required to accurately

Table 1. Histopathologic grading based on the invasive front grading system for squamous cell carcinomas (Dissanayake, 2017).

Morphologic parameters	Scores			
	1	2	3	4
Degree of keratinization	Highly (>50%)	Moderately (20-50%)	Minimal (5-20%)	No (0-5%)
Nuclear pleomorphism	Little	Moderately	Abundant	Extreme
Number of mitoses ^a	0-1	2-3	4-5	>5
POI	Pushing borders	Infiltrating cords/bands or strands	Small cell groups (n > 15)	Single cells/tiny groups (n < 15)
Lymphocytic infiltration	Marked	Moderate	Slight	None

^a per high power field

^b POI: pattern of invasion

distinguish between a benign hamartoma and a SCC.

The metastasis rates for feline SCC vary (0% to 36%), with regional lymph nodes being common sites (Hutson et al., 1992; Gendler et al., 2010). No lymph node enlargement was noted in this case, but metastatic disease cannot be excluded based on this alone. Sentinel lymph node mapping aids in exclusion, in which CT, ultrasound, fluoroscopy or lymphoscinti-graphy can be used as diagnostic tools. When using CT, ultrasound, or lymphoscintigraphy, the lymph node mapping is performed before surgical excision, while fluoroscopy can be performed intraoperatively. The primary lymph node where uptake is seen, is designated as the sentinel lymph node, and should be excised or subjected to biopsy, followed by histopathological examination. Another possibility are fine-needle aspirations of the sentinel lymph node, although histopathology is considered the gold standard, while cytological examination can still yield a significant rate of false negative results (Herring et al., 2002).

CT imaging provides crucial information about oral masses, including size, margin, characteristics, contrast enhancement and aiding in metastatic spread evaluation. Despite lacking specificity, CT remains vital in the diagnostic process.

In conclusion, given the challenges in definitively distinguishing benign lesions from SCC based on imaging alone, histopathological diagnosis remains essential. A comprehensive approach combining clinical, radiological and histopathological assessments is crucial for the accurate management of cats with oral lesions.

LITERATURE

Bilgic O., Duda L., Sanchez M.D., Lewis J.R. (2015). Feline oral squamous cell carcinoma: Clinical manifestations and literature overview. *Journal of Veterinary Dentistry* 32, 30-40.

- Dissanayake U. (2017). Malignancy grading of invasive fronts of oral squamous cell carcinomas; Correlation with overall survival. *Translational Research in Oral Oncology*. Volume 2. <https://doi.org/10.1177/2057178X17708>
- Herring E.S., Smith M.M., Robertson J.L. (2002). Lymph node staging of oral and maxillofacial neoplasms in 31 dogs and cats. *Journal of Veterinary Dentistry* 19(3), 122-174.
- Gendler A., Lewis J.R., Reetz J.A., Schwarz T. (2010). Computed tomographic features of oral squamous cell carcinoma in cats: 18 cases (2002-2008). *Journal of American Veterinary Medical Association* 236, 319-325.
- Harvey C.E., Emily P. (1993). Oral neoplasms. In: Harvey C.E. and Emily P. (editors). *Small Animal Dentistry*. St. Louis, Mosby, pp. 306.
- Hayes A.M., Adams V.J., Scase T.J., Murphy S. (2007). Survival of 54 cats with oral squamous cell carcinoma in United Kingdom general practice. *Journal of Small Animal Practice* 48, 394-399.
- Hutson C.A., Willauer C.C., Walder E.J., Stone J.L., Klein M.K. (1992). Treatment of mandibular squamous cell carcinoma in cats by use of mandibulectomy and radiotherapy: seven cases (1987-1989). *Journal of American Veterinary Medical Association* 201, 777-781.
- Král D., Pink R., Šašková L., Michálek J., Tvrdý P. (2021). Bone invasion by oral squamous cell carcinoma. *Journal of Plastic Surgery (Acta Chirurgiae Plasticae)* 63(3), 139-144.
- Liptak J.M., Withrow S.J. (2007). Oral tumors. In: *Small Animal Clinical Oncology*. Liptak J.M. and Withrow S.J. (editors). Fourth edition, St Louis, Saunders Elsevier, 455-478.
- Martin-Vaquero P., Moore S.A., Wolk K.E., Oglesbee M.J. (2011). Cerebral vascular hamartoma in a geriatric cat. *Journal of Feline Medicine and Surgery* 13, 286-290.
- Murphy B.G., Bell C.M., Soukup J. (2020). Oral squamous cell carcinoma. In: Murphy B.G., Bell C.M. and Soukup J. (editors). *Veterinary Oral and Maxillofacial Pathology*. First edition, Hoboken, NJ, Wiley & Sons, pp. 139-148.
- Nemanic S., London C.A., Wisner E.R. (2006). Comparison of thoracic radiographs and single breath-hold helical CT for detection of pulmonary nodules in dogs with metastatic neoplasia. *Journal of Veterinary Internal Medicine* 21(1), 27-31.

- Padgett S.L., Tillson D.M., Henry C.J., Buss M.S. (1997). Gingival vascular hamartoma with associated paraneoplastic hyperglycemia in a kitten. *Journal of American Veterinary Medical Association* 210, 914-915.
- Panarese I., Aquino G., Ronchi A., Longo F., Montella M., Cozzolino I., Rocuzzo G., Colella G., Caraglia M., Franco R. (2019). Oral and Oropharyngeal squamous cell carcinoma: prognostic and predictive parameters in the etiopathogenetic route. *Expert Review of Anticancer Therapy* 19(2), 105-119.
- Pavlin D., Dolenssek T., Švara T., Nemeč A. (2018). Solid type primary intraosseous squamous cell carcinoma in a cat. *BMC Veterinary Research* 14(1), 23.
- Postorino Reeves N.C., Turrel J.M., Withrow S.J. (1993). Oral squamous cell carcinoma in the cat. *Journal of the American Animal Hospital Association* 29, 438-441.
- Sigal R., Zagdanski A.M., Schwaab G., Bosq J., Auperin A., Laplanche A., Francke J.P., Eschwège F., Luboinski B., Vanel D. (1996). CT and MR imaging of squamous cell carcinoma of the tongue and floor of the mouth. *Radiographics* 16, 787-810.
- Smith T.J., Baltzer W.I., Ruaux C.G., Heidel J.R., Carney P. (2010). Gastric smooth muscle hamartoma in a cat. *Journal of Feline Medicine and Surgery* 12, 334-337.
- Soltero-Rivera M.M., Krick E.L., Reiter A.M., Brown D.C., Lewis J.R. (2014). Prevalence of regional and distant metastasis in cats with advanced oral squamous cell carcinoma: 49 cases (2005-2011). *Journal of Feline Medicine and Surgery* 16(2), 164-169.
- Stebbins K.E., Morse C.C., Goldschmidt M.H. (1989). Feline oral neoplasia: a ten-year survey. *Veterinary Pathology* 26, 121-128.
- Strohmayr C., Klang A., Kneissi S. (2010). Computed tomographic and histopathological characteristics of 13 equine and 10 feline oral and sinonasal squamous cell carcinomas. *Frontiers Veterinary Science* 7, 591437.
- Subsavhad W., Dirksen W.P., Martin C.K., Rosol T.J. (2016). Animal models of head and neck squamous cell carcinoma. *The Veterinary Journal* 210, 7-16.
- Takagi S., Kagawa Y., Hanazono K., Murakami S., Deguchi T., Izumi Y., Hosoya K., Kim S., Okumura M. (2018). Mandibular vascular hamartoma in a cat. *Journal of Veterinary Medicine and Science* 80(9), 1456-1458.
- Tsuka T., Okamoto Y., Yamamoto N., Hayashi K., Morita T., Sunden Y., Murahata Y., Azuma K., Osaki T., Ito N., Imagawa T. (2018). Unilateral rostral mandibulectomy for gingival vascular hamartoma in two calves. *Journal of Veterinary Science* 19, 582-584.



© 2024 by the authors. Licensee Vlaams Diergeneeskundig Tijdschrift, Ghent University, Belgium. This article is an open access article distributed under the terms and conditions of

the Creative Commons Attribution (CC BY) license (<http://creativecommons.org/licenses/by/4.0/>).